Flat Fading Channel Simulation

Mitchell Kiner

I. Introduction

In wireless communication, the signal strength at a receiver or antenna varies significantly due to multiple physical phenomena. There are two key effects that cause these variations in signal strength, referred to as shadowing and fading. Shadowing, also known as slow fading, refers to attenuation of a signal caused by large obstacles such as buildings, hills, or trees. Shadowing results in local average signal fluctuations over distances of tens to hundreds of meters. In contrast, fast fading, particularly multipath fading, is caused by the presence of multipath propagation, where multiple copies of the same signal arrive at the receiver from various paths with different delays and phases. This causes rapid fluctuations in amplitude and phase over short distances or time intervals. Fig. 1 shows examples of how shadowing and multipath fading can occur in a wireless channel. When designing wireless communication systems, understanding and accurately simulating/estimating these effects is crucial for a reliable connection.

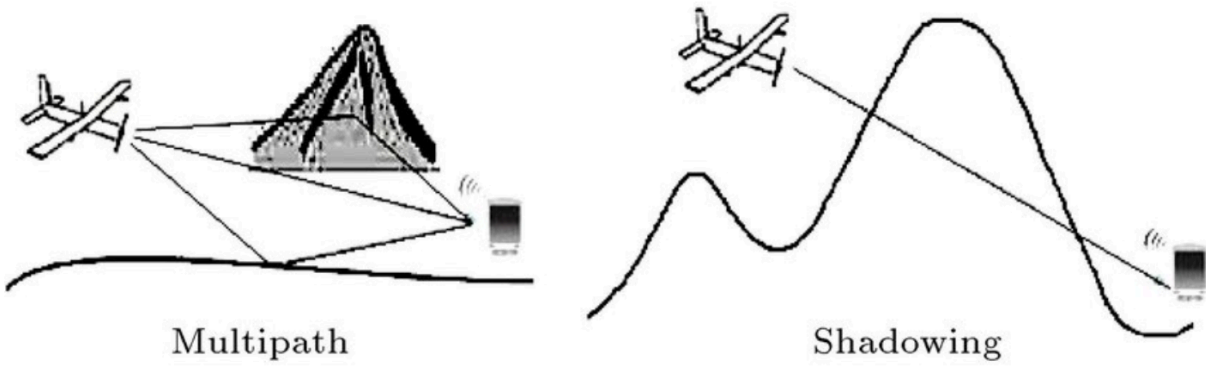

Fig. 1 (Dehghan & Moradi 2016): Physical representations of multipath fading and shadowing. In multipath fading, reflections off of different surfaces are causing multiple copies of the same signal to arrive at the receiver, whereas shadowing is caused by the presence of obstacles in between the receiver and transmitter, affecting the direct signal path.

II. Scenario

For this simulation, an outdoor, urban setting has been chosen, commonly characterized by moderate to severe multipath effects, structural obstructions (particularly large buildings), and NLOS (non-line-of-sight) conditions, meaning that the transmitted signal does not have a direct path to the receiver.

Because of the NLOS conditions chosen, the envelope of the received signal follows a Rayleigh distribution. On top of this, movement of the receiver (i.e. driving with your phone) will introduce a Doppler shift to the received signal. These conditions

are commonly referred to as Rayleigh fading and further inform the choice of parameters below:

1. **Path Loss Exponent:**
    a. Urban environments typically exhibit a path loss exponent between 2.7 and 4 due to diffraction and scattering. An exponent of 3.5 represents a realistic scenario where mostly NLOS paths contribute to the received signal.
2. **Standard Deviation of Shadowing:**
    a. From empirical path loss models, like the Hata model, we find that a standard deviation of 8 dB for shadowing is typical for outdoor urban environments with larger obstructions (Behbahani 2025).
3. **Doppler Frequency:**
    a. The Doppler frequency was set assuming a user speed of approximately 30 km/h, which is typical for a car in an urban environments, and a carrier frequency around 900 MHz (e.g. GSM band). This results in a maximum Doppler shift of around 83 Hz.

III. Channel Modeling

With the parameters of this simulation selected, the channel can now be accurately modeled. To understand how each channel component (path loss, shadowing, and Rayleigh fading) affects the received signal, the simulation presents a series of outputs progressively incorporating each impairment:

1. **Path Loss**

Path loss captures a signal's attenuation due to distance, where $d_0 = 1$ meter is a reference point and $\alpha = 3.5$ is the path loss exponent selected for this simulation. With these inputs, path loss can be modeled using the log-distance path loss model (Behbahani 2025):

$$PL(d) = PL(d_0) + 10\alpha log_{10}(\frac{d}{d_0}) \quad (1)$$

Since the focus of this simulation is relative path loss, and how it grows with distance, $PL(d_0)$ can be defined as 0 dB and treated as a baseline. Fig. 2 shows the path loss model according to equation 1:

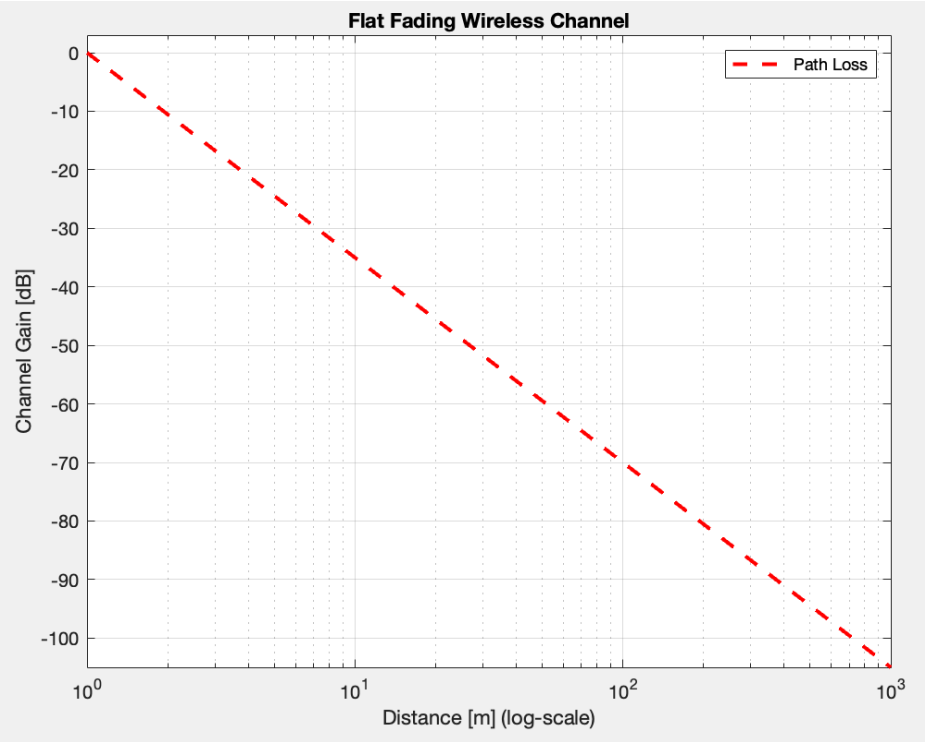

Fig. 2: Path loss model with path loss exponent $\alpha = 3.5$. Since the x-axis is in log-scale, the log-distance path loss model is represented linearly. As the distance between the transmitter and receiver increases, so does the channel loss (negative gain).

This model represents an ideal channel, meaning there is no additional noise incorporated. In reality, thermal and environmental noise corrupts the channel, introducing random fluctuations around the ideal path loss curve. This can be simulated with additive white Gaussian noise (AWGN). The received signal then becomes:

$$y = \sqrt{PL(d)} + n(t) \tag{2}$$

where $n(t)$ is complex Gaussian noise with zero mean and σ^2 variance. The received power is then measured as:

$$P = |y|^2$$

Fig. 3 compares the path loss model with and without AWGN in the channel. It is apparent that introducing AWGN creates what is referred to as a noise floor, setting the lower bound for signal detection and limits the system's sensitivity and dynamic range. In a wireless system, the noise floor includes thermal noise and other unwanted signals like interference, receiver imperfections, and quantization noise.

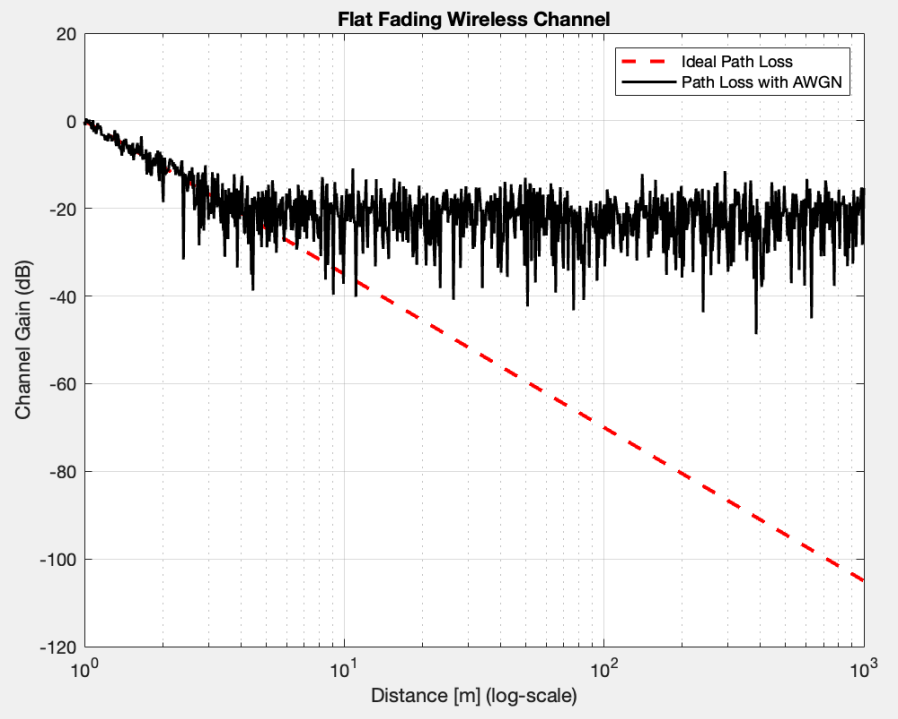

Fig. 3: Comparison of path loss model with path loss exponent $\alpha = 3.5$ and path loss model with AWGN zero mean and 0.01 variance (equation 2).

Although including AWGN provides a more realistic simulation of a wireless channel, it will make it more difficult to compare the effects of shadowing and Rayleigh fading on the channel, so the rest of the simulation will not include AWGN and use the ideal path loss model.

2. Shadowing

Shadowing can be modeled by adding a multiplicative log-normal term to the ideal path loss model (Behbahani 2025):

$$SF(d) = PL(d) + X_{\sigma} \tag{3}$$

where $X_{\sigma} \sim N(0, \sigma_{sf}^{2})$.

Fig. 4 overlays the effects of shadowing according to equation 3 over the ideal path loss model (equation 1), showing how shadowing results in a more realistic curve that varies smoothly due to environmental obstructions, like large buildings in this case. Fig. 5 provides a zoomed in view of the same plot in Fig. 4, making the rate and amplitude of these fluctuations more apparent. The rate at which these oscillations cross over the ideal path loss model give rise to the name “slow fading”, since variations in the channel occur over longer distances.

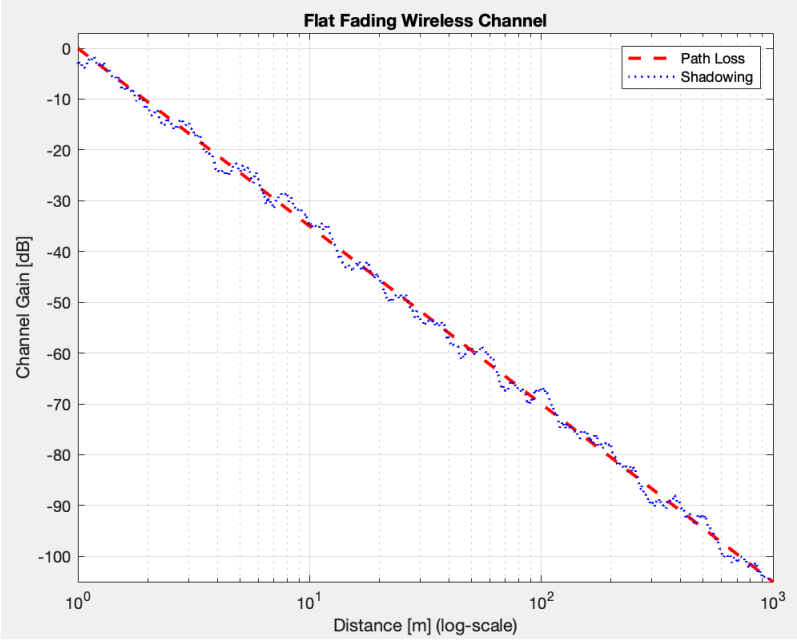

Fig. 4: Shadowing model with shadowing standard deviation $\sigma_{sf}^{\ 2} = 8\,dB$ plotted over ideal path loss model with path loss exponent $\alpha = 3.5$.

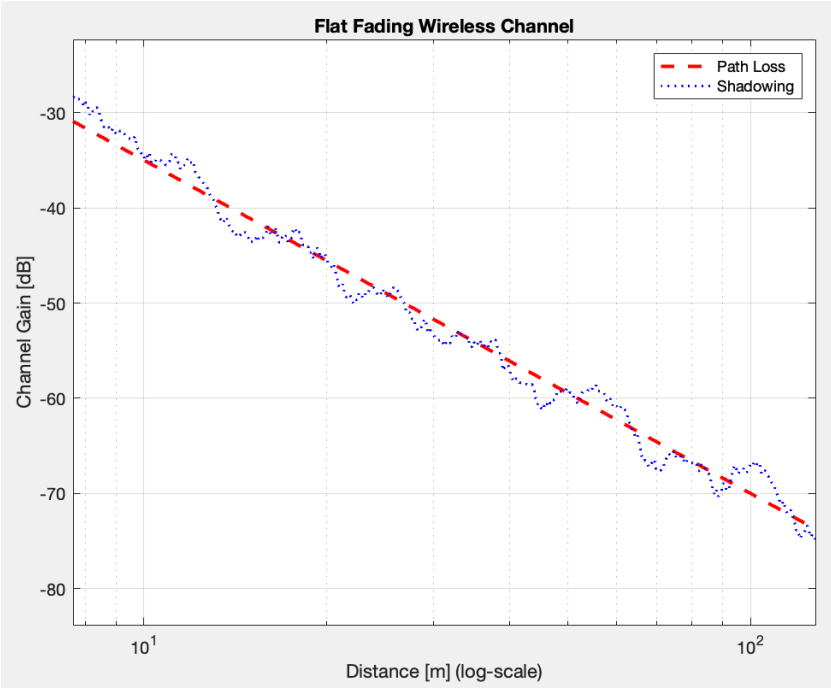

Fig. 5: Zoomed view of Fig. 4, focusing on distances from 10 meters to 100 meters between transmitter and receiver.

3. Rayleigh Fading

Rayleigh fading can be added to the simulation by using the Clarke model (Behbahani 2025). The Rayleigh fading envelope is generated by:

$$r(t) = \left|\Sigma^{M}_{m=1} exp(j(\omega_d cos(\theta_m)t + \phi_m))\right| \quad (4)$$

Here, M is the number of sinusoids used in the Clarke model to approximate the Doppler effect. Each sinusoid represents a different multipath component arriving at a different angle and with a random initial phase. The approximation to the theoretical Doppler spectrum depends on the value of M selected. For this simulation, $M = 64$.

The envelope $r(t)$ is normalized to have unit power, and the final received signal can be represented by:

$$y = \sqrt{SF(d)} \cdot r(t)$$

and again, the power at the receiver is:

$$P = |y|^2$$

Fig. 6 overlays the effects of Rayleigh fading according to equation 4 over the ideal path loss model (equation 1), as well as shadowing (equation 3). Fig. 7 provides a zoomed in view of the same plot in Fig. 6, making the rate and amplitude of these fluctuations more apparent. The rate at which these oscillations cross over the shadowing model give rise to the name "fast fading", since variations in the channel occur over shorter distances.

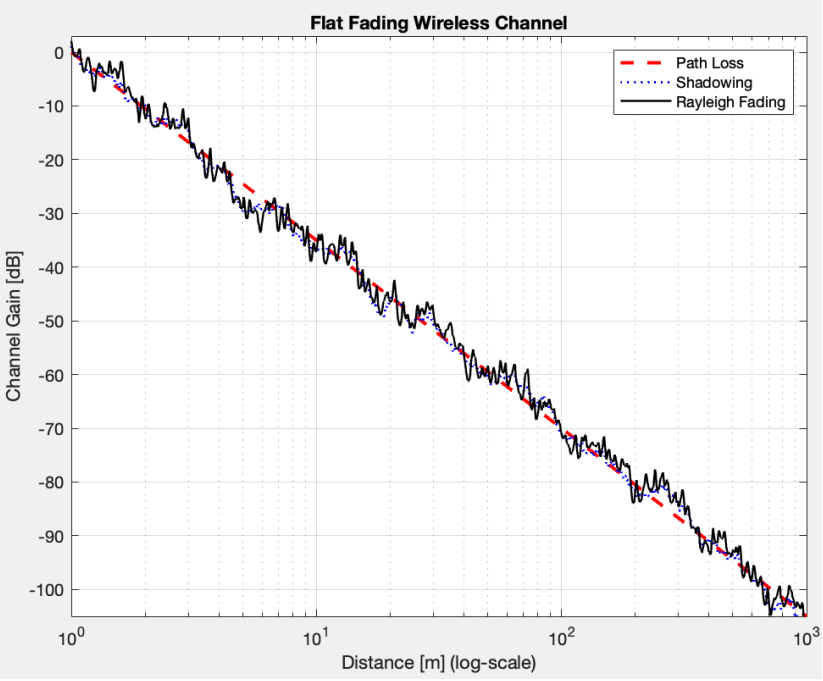

Fig. 6: Rayleigh fading with maximum Doppler shift of 83Hz plotted over shadowing model with shadowing standard deviation $\sigma_{sf}^2 = 8dB$ and ideal path loss model with path loss exponent $\alpha = 3.5$.

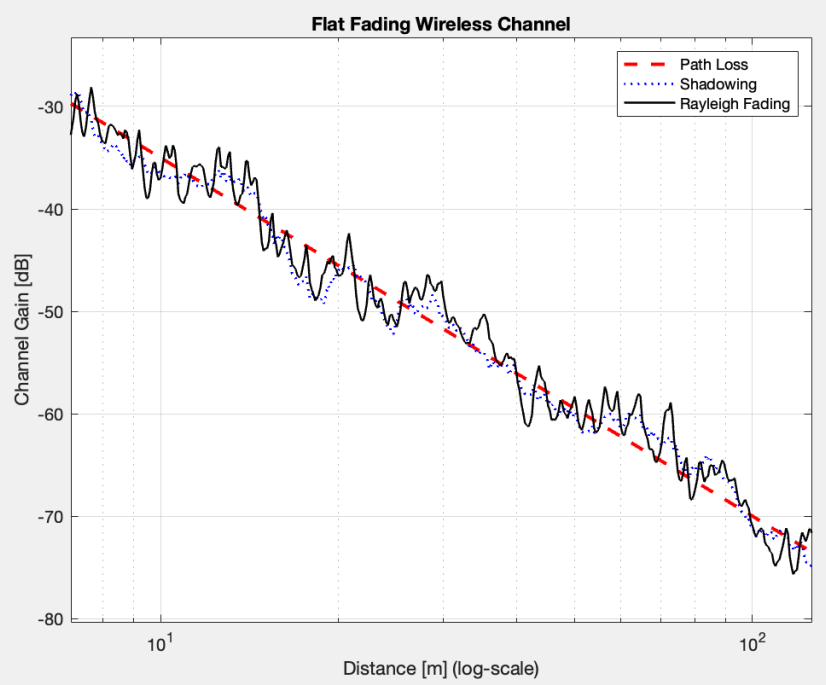

Fig. 7: Zoomed view of Fig. 6, focusing on distances from 10 meters to 100 meters between transmitter and receiver.

From Fig. 7, it is easier to see how variations in receiver power due to Rayleigh fading rapidly fluctuate around the shadowing model, while still following the overall trend of the ideal path loss model. This is why Rayleigh fading is sometimes referred to as the "full path model" since it takes into account all the different types of path loss and fading (slow and fast) present in the channel.

IV. Verifying the Simulation

---

1. Shadowing Probability Density Function (PDF)

In the simulation, shadow fading was generated as a Gaussian random process with standard deviation 8 dB. The PDF of this can be represented by the standard normal distribution:

$$P(x) = \frac{1}{\sigma\sqrt{2\pi}} e^{-\frac{x^2}{2\sigma^2}} \quad (5)$$

Fig. 8 compares the theoretical PDF in equation 5 to the number of spatial points whose shadowing gain (in dB) falls within each bin of the histogram.

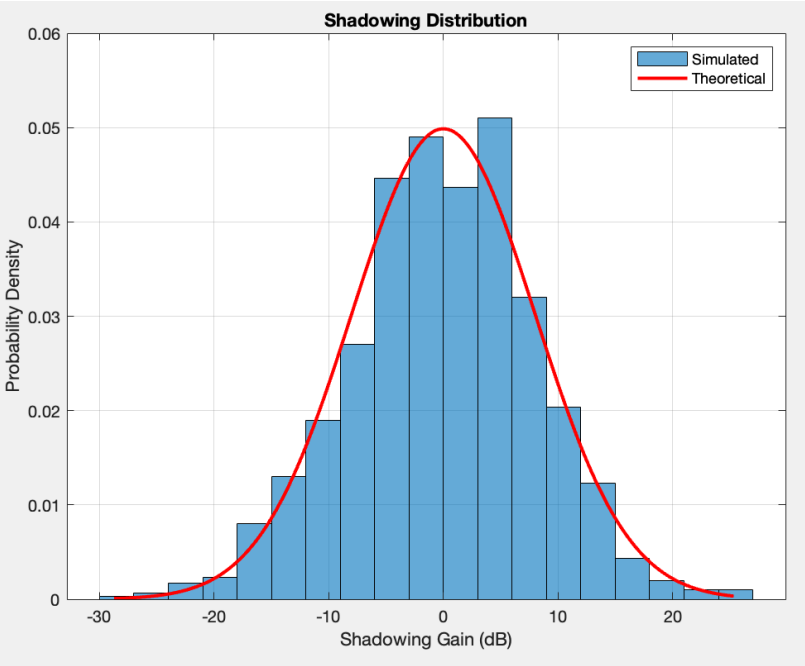

Fig. 8: Theoretical vs. simulated PDF of shadowing.

The histogram of the simulation closely follows the bell curve shape, validating that the shadowing process was correctly implemented. To enhance the alignment, a larger number of spatial samples (i.e., simulate over a longer distance) can be generated. Additionally, applying a smoother window to the shadowing generation or reducing histogram bin width can also increase resolution. The use of a true low-pass filter or correlated log-normal model may further improve physical realism as well.

2. Rayleigh Envelope PDF

The theoretical PDF Rayleigh processes can be defined by the Rayleigh distribution:

$$P(r) = \frac{r}{\sigma^2} e^{-\frac{r^2}{2\sigma^2}}, \quad r \geq 0 \tag{6}$$

σ can be chosen to be $\frac{1}{\sqrt{2}}$ so that the mean power is 1.

Fig. 9 compares the theoretical PDF in equation 5 to the distribution of the normalized fading envelope amplitudes across the simulation duration. Each bin counts how many amplitude values fall within that range.

The histogram of the simulation closely aligned with the theoretical PDF of the Rayleigh distribution, especially around the mean, confirming that the simulated fast fading replicates the statistical behavior expected from Rayleigh processes.

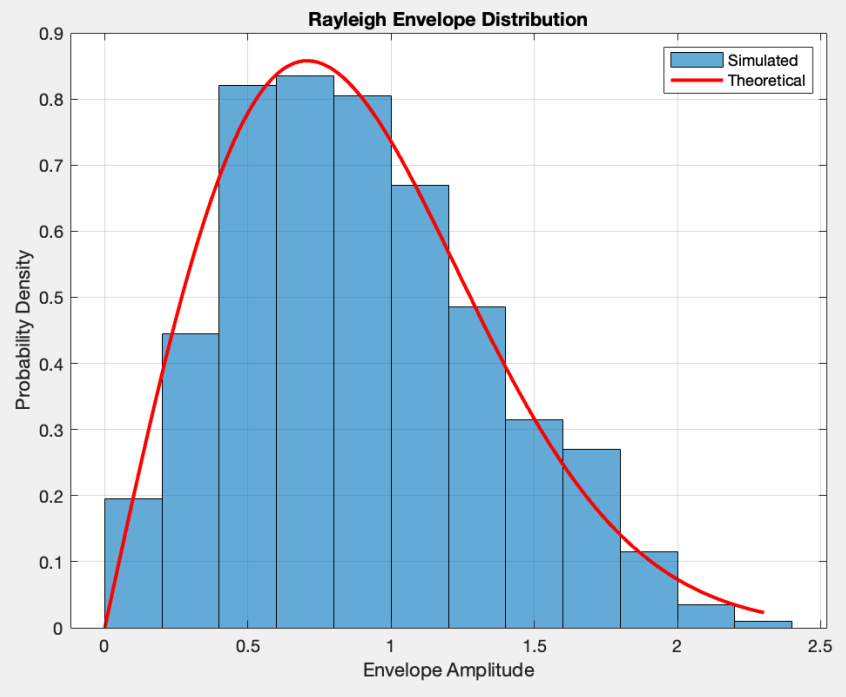

Fig. 9: Theoretical vs. simulated PDF of Rayleigh fading.

To bring the simulated histogram even closer to the theoretical PDF, the number of fading samples (i.e., simulate over longer distances or higher sampling rate) can be increased or the number of bins in the histogram can be increased for finer resolution. Increasing the number of sinusoids M in the Clarke model (e.g., to 100 or more) also helps improve the statistical realism of the Rayleigh process.

3. Power Spectral Density (PSD) of Rayleigh Fading vs. Jakes' Spectrum

Another way to validate this simulation is to compare the PSD of the simulated Rayleigh fading to Jakes' spectrum. Jakes' spectrum describes the theoretical power spectral density (PSD) of a Rayleigh fading signal in a flat fading wireless channel due to Doppler spread. It assumes uniform distribution of arrival angles for multipath components and isotropic scattering around a moving receiver (Jakes 1975). Jakes' spectrum is defined by the equation:

$$S(f) = \frac{1}{\pi f_d \sqrt{1-\left(\frac{f}{f_d}\right)^2}}, \quad |f| < f_d \tag{7}$$

where f_d refers to the maximum Doppler shift, which was 83 Hz in the simulation.

Using Welch's method, an estimate of the PSD of the Clarke model based simulation of Rayleigh fading can be found. Fig. 10 plots the estimated PSD against Jakes' spectrum.

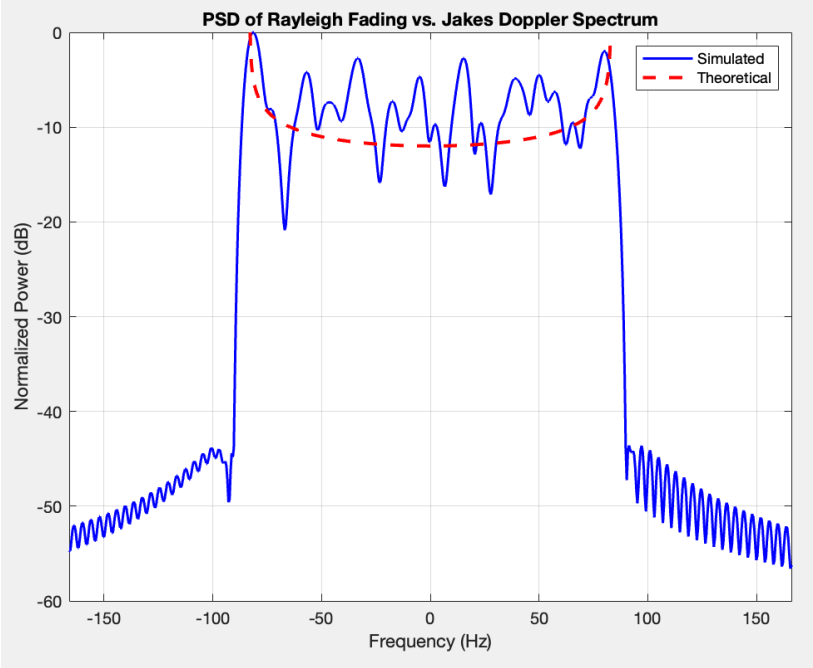

Fig. 10: Estimated PSD of simulated Rayleigh fading with the Clarke model vs. Jakes' spectrum, maximum Doppler shift (f_d) of 83 Hz.

The goal of this validation is to confirm that the simulated Rayleigh fading exhibits the expected spectral shape, a key indicator that the Doppler characteristics of the channel have been modeled correctly. Jakes' spectrum serves as the theoretical benchmark for Rayleigh fading in isotropic scattering environments.

When comparing the simulated PSD with the theoretical Jakes' spectrum, we observe that the overall U-shape of the spectrum is well captured. The main lobe aligns in bandwidth and shape, indicating the simulation's Doppler characteristics are correct. However, the simulated PSD exhibits more spectral ripples and variance, especially near the edges of the Doppler bandwidth ($\pm f_d$). This is expected due to the finite number of sinusoids (M) used and the statistical nature of the Welch estimation. Increasing the number of sinusoids in the Clarke model would improve the smoothness and accuracy of the simulated Doppler spectrum. Additionally, tuning the parameters of Welch's method (such as window length, overlap, and FFT size) can also result in better frequency resolution and lower variance in the estimated PSD.

V. Conclusion

This simulation successfully models a flat fading wireless channel with realistic parameters for an outdoor, urban scenario. The shadowing and Rayleigh components

were verified both statistically and spectrally. This simulation could easily be modified to simulate other scenarios as well, like suburban and rural environments, where LOS conditions may be more achievable, or different motions of the receiver (like freeway speeds). This would be done with changes to the parameters outlined in Section II: the path loss exponent, standard deviation of shadowing, and Doppler frequency. On top of this, this setup can be extended further for bit-error rate (BER) analysis, diversity studies, or mobility modeling of different channel conditions, all of which are crucial when designing accurate wireless communication systems.

Despite this, the most glaring limitation of this simulation is that the wireless channel is modeled as a 1D spatial process; channel properties like path loss, shadowing, and Rayleigh fading are computed as functions of distance from the transmitter. While this provides a clear and computationally efficient view of fading effects, it does not capture angular dynamics or spatial correlation across multiple dimensions. Future extensions could explore 2D or 3D receiver trajectories, incorporate directionality of scatterers, or model antenna arrays to better represent real-world multipath environments and MIMO scenarios.

VI. References

1. Behbahani, A.S. (2025, May). Wireless Communication Channel [PowerPoint slides]. Department of Electrical Engineering and Computer Science, University of California, Irvine.

2. Dehghan, S.M.M. & Moradi, Hadi. (2016). A multi-step Gaussian filtering approach to reduce the effect of non-Gaussian distribution in aerial localization of an RF source in NLOS condition. Scientia Iranica. 23. 2682-2693. 10.24200/sci.2016.3977.

3. Jakes, W. C. (Ed.). (1975). Microwave mobile communications. John Wiley & Sons.